Lymphoreticular and Myeloid Pathogenesis of Venezuelan Equine Encephalitis in Hamsters

David H. Walker, MD, Alyne Harrison, BS, Kevin Murphy, MD, Mary Flemister, MS, and Frederick A. Murphy, DVM, PhD

Ultrastructural, histopathologic, and virologic studies of adult hamsters infected with virulent Venezuelan equine encelphalomyelitis (VEE) virus (Subtype I-B) demonstrated precise chronologic and topographic progression of lesions and viral replication in extraneural sites. Thymus contained the earliest lesions and the highest initial and subsequent viral titers. No particular cytotropism was observed as highly efficient viral replication and severe cytonecrosis proceeded. Early cortical necrosis of splenic periarteriolar lymphocytic sheath was followed by lymphoblastoid repopulation of the peripheral zone. Massive bone marrow necrosis was accompanied by ultrastructural evidence of VEE viral particle production in reticulum cells, rubricytes, myeloid cells, lymphoblastoid cells, and megakaryocytes. Speed, efficiency, destructiveness, and relative sensitivity of virtually all lymphoreticular and hematopoetic cells were hallmarks of virulent VEE infection in the hamster. (Am J Pathol 84:351–370, 1976)

TWO MAJOR pathogenetic patterns are exhibited by the various alphaviruses (the Group A arboviruses) in their mammalian hosts. One pattern, that of predominant neurotropism, is exemplified by eastern equine encephalitis virus.[1] This pattern depends upon minimal extraneural viral proliferation and rapid destructive infection of the central nervous system. A second pattern, that of predominant myotropism, is exemplified in experimentally infected mice by Ross River virus [2] and in man, probably by chikungunya virus. In this pattern, despite a high viremia, invasion of the central nervous system is minimal. Most of the other alphaviruses have pathogenetic patterns in experimentally or naturally infected mammals and man that fit one of these patterns or a combination of the two. However, one exceptional pattern is represented by Venezuelan equine encephalitis (VEE) virus in hamsters and guinea pigs.[3-7] *In vivo* studies in these species have shown lymphoreticulotropism and myelotropism. In some species, such as the mouse,[8,9] horse,[10] and monkey,[11] the extraneural sites of viral growth contribute to lethal invasion of the central nervous system, but in the hamster and the guinea pig, death occurs rapidly and precedes evidence of neurologic disease. The lymphoreticular and myeloid tissue destruction in these species is

From the Center for Disease Control Public Health Service, US Department of Health, Education, and Welfare, Atlanta, Georgia.

Accepted for publication April 5, 1976.

Address reprint requests to Dr. David H. Walker, Department of Pathology, University of North Carolina, School of Medicine, Chapel Hill, NC 27514.

massive. Several histopathologic descriptions of this destruction of bone marrow, splenic white pulp, thymus, and lymph nodes have been published. At the ultrastructural level, study of the extraneural pathogenesis of VEE virus infection in hamsters has been limited to Peyer's patches [12] and pancreas.[13]

The acutely lethal mechanisms involved in viral destruction of lymphoreticular and myeloid tissues must be extremely complex; in a recent contribution to our understanding of these mechanisms, necrotizing infection of Peyer's patches in hamster ileum was shown to result in bacteremia, increased sensitivity to bacterial endotoxin, and terminal endotoxin-induced shock.[12] In this context, death is related to viral destruction of only one lymphoreticular organ, but destruction of all such organs occurs, and the entire capacity of the host to mount immunologic and reticuloendothelial defense is compromised.

The present study was undertaken to extend understanding of the ultrastructural events in several lymphoreticular and myeloid elements of hamsters infected with a virulent strain of VEE virus. Toward this end, thymus, spleen, and lymph nodes (and ileum) of infected hamsters were serially studied by infectivity titration and by light and electron microscopy.

Materials and Methods

Virus and Viral Assay

VEE virus (Subtype I-B; strain designation "Three Rivers," CDC W37947), obtained as a third suckling mouse brain passage, was diluted 10^{-6} in 0.75% bovine albumin phosphate-buffered saline (BAPS) for animal inoculation. Two-tenths milliliter of this diluted stock contained 100 plaque-forming units (PFU) of virus. Organ and tissue infectivity titrations on samples of plasma, spleen, thymus, lymph node, and Peyer's patch were assayed by plaquing in primary duck embryo cell cultures maintained under agar medium according to a standard method.[14] Infectious virus content of these organs and tissues is expressed as plaque-forming units per gram of tissue or milliliter of fluid.

Animals

Twenty-one 8-week-old male LVG:LAK Syrian hamsters (Lakeview Hamster Colony, Charles River Company, Newfield, N. J.), were inoculated subcutaneously with 100 PFU of VEE virus contained in 0.2 ml.

Experimental Design

Tissue specimens were collected from animals killed and exsanguinated at 8, 24, 48, and 72 hours after inoculation. Specimens were also collected from 2 remaining animals which died on the fourth day after inoculation (for histopathology only). Tissues from each animal were divided for infectivity titration, light microscopic histopathology, and thin section electron microscopy.

Histopathology

Thymus, lymph node, spleen, bone marrow, and small bowel were fixed in 10% neutral buffered formalin, dehydrated in alcohol, embedded in paraffin, sectioned at 6 μ, and stained with hematoxylin and eosin. Tissues from 7 animals killed on Days 1, 2, and 3 were stained by the Brown-Brenn method for bacteria, by periodic acid–Schiff's stain, or by reticulin stains. Lymph nodes from 10 animals were fixed in Carnoy's solution and processed for staining with methyl green–pyronin.

Electron Microscopy

Samples of thymus, spleen, lymph node, bone marrow, and ileum were fixed in 2.5% buffered glutaraldehyde for 2 hours, washed in a phosphate buffer, postfixed in 1% osmium tetroxide, dehydrated in a graded alcohol series, and embedded in an Araldite-Epon mixture.[15] Sections were stained with uranyl acetate and lead citrate [16] and were examined in Philips 300 and Philips 200 electron microscopes.

Results

Thymus

On the first day after inoculation, thymic structure of infected mice did not differ appreciably from that of uninoculated controls. However, diffusely scattered throughout both the cortex and medulla were individual cells which were rounded and shrunken and had pyknotic nuclei. Fewer than 1% of the cells in the thymus were involved, but this change was seen in all specimens. Because of the magnitude of normal cell turnover in thymus, the inoculated controls were reexamined, but this change was never seen in them. Ultrastructurally, no evidence of viral infection or cytopathic changes was observed at this time.

On the second day after inoculation, focal necrosis of thymocytes and epithelial reticular cells was observed. Lesions were present in two forms. One form consisted of rounded, "punched out" foci of cells with pyknotic nuclei intermixed with nucleorrhectic debris and lucent space (Figure 1). These foci had precise edges, producing a "Swiss cheese effect." The other form of focal necrosis consisted of irregular masses of pyknotic cells without lucent surrounding space or precise separation from normal surrounding cells (Figure 2). The cortex and medulla of thymic specimens were affected equally, but the "punched out" form of the necrotic lesion was more obvious in the cortex. Light microscopy indicated that, overall, 25% of the thymus was involved in these necrotic changes.

Ultrastructurally, typical VEE virus particles were observed budding from the plasma membranes of small thymocytes (Figure 3), large lymphoblastoid cells (Figure 4), and epithelial reticular cells (Figure 5). Viral nucleocapsids were found only infrequently in these cells at sites near

viral budding (Figure 6); the lack of accumulation of nucleocapsids is considered evidence of a high degree of efficiency of the budding process and production of infectious virus.

In relation to the infectivity titer of thymus at this time (Table 1), viral budding was observed infrequently, and inordinately few virus particles were found in extracellular spaces. Thymus at 2 days postinoculation had the highest virus titer found in any hamster tissue at any time. This dilemma has been observed in other *in vivo* studies of VEE, but remains unexplained.[17]

The ultrastructural necrotic changes involved thymocytes and epithelial reticular cells (Figure 7), with no apparent difference in the resistance of the two types of cells to the damaging aspects of infection. At the margins of necrotic foci, there was a rather sharp line demarcating intact and necrotic cells, and there was no deviation in this line when the demarcation was formed by either lymphoid or reticular elements. Virus particles were trapped amid the necrotic debris filling these foci. Phagocytosed virus particles were also present within vacuoles of some polymorphonuclear (PMN) leukocytes. Capillaries near areas of necrosis contained necrotic debris in their lumina as well as circulating virus particles. The latter is consistent with the very high level of viremia (Table 1).

By Day 3, foci of necrotic cells had enlarged and, in many instances, had coalesced; necrotic changes involved approximately 60% of the mass of the thymus. As previously noted, margins between necrotic and viable cells could be demarcated, but at this stage, islands of normal cells were surrounded by necrotic cells. Because of the presence of large numbers of pyknotic nuclei, many necrotic areas did not appear completely acellular, but cell density did seem decreased. Even the relatively resistant Hassal's corpuscles were focally necrotic. As was observed earlier, the cortex and medulla and the lymphoid and reticular elements were uniformly destroyed (Figure 8). Electron microscopy indicated that many more thy-

Table 1—Organ Infectivity Titers From Adult Hamsters Inoculated With Venezuelan Equine Encephalitis Virus

Animal	Day of sacrifice	Plasma	Thymus	Spleen	LN
A	2	7.3	9.2	8.2	6.6
B	2	7.0	8.9	7.7	7.8
C	3	ND	8.2	8.1	8.0
D	3	5.6	8.6	7.9	7.8

ND = not done.
Values are log plaque-forming units per gram of tissue or milliliter of fluid.

mocytes and epithelial reticular cells were damaged by viral infection than was evident by light microscopy, but there was no qualitative difference in morphologic findings from those described for Day 2.

Thymus from animals found dead on Day 4 had massive necrosis with focal islands of individual or small groups of viable cells. Cortex and medulla were both severely involved, and all cell types (thymocytes, epithelial reticular cells, and Hassal's corpuscles) were destroyed. An estimated 90, 70, and 50% of these cell types, respectively, had undergone necrotic changes. This differential resistance of both the highly differentiated epithelial cells of Hassal's corpuscles and the epithelial reticular cells was only evident at the time of death because of the cumulative relative sensitivity of the thymic lymphocyte population.

Lymph Nodes

On Day 1 postinoculation, lymph node architecture was intact; in this age hamster, nodes consisted of a cortex containing several (usually about six) follicles, a paracortical zone of moderate size (occupying up to one-third of the volume of the node), and a large medulla consisting of medullary cords (containing plasmacytoid lymphocytes, plasma cells, and a few eosinophils) and sinuses with few intraluminal lymphocytes and macrophages. By Day 2, lymph nodes had necrotic cortical follicles and scattered nucleopyknosis of plasma cells in medullary cords. In many nodes, the cortical lymphoid necrosis was confluent (Figure 9); by contrast, the relative sparing of the medullary elements was quite apparent. By electron microscopy, virus particles were found free in many of the interstitial spaces; they were in highest concentrations in perivascular spaces in association with all layers of basement lamina. Virus particles were also prominent near fibroblasts, being trapped amid collagen bundles. Fewer virus particles were observed budding from lymphocytes and reticulum cells than in the thymus, and intracellular virus particles and nucleocapsids were rare. Very few virus particles were found within vacuoles of endothelial cells. By Days 3 and 4, necrosis of the cortex and parcortical region of nodes were so nearly complete that anatomic distinction of follicles and other structures was effaced. The surviving cortical cells were large lymphoblasts and mononuclear cells. The medullary cords contained approximately half necrotic and half viable cells; the latter consisted mainly of plasmacytoid lymphocytes and plasma cells. Ultrastructurally, lymph nodes from animals sacrificed 3 days after inoculation contained massive areas of cytonecrosis; extracellular virions were predominantly enmeshed in cytoplasmic debris.

Spleen

Spleen showed no histopathologic changes until 2 days after virus inoculation, at which time necrosis of cells was observed within the periarteriolar lymphocytic sheath (PALS). In many instances, the necrosis tended to involve the periphery of the PALS with relative sparing of cells near the central arteriole. This was especially evident where the plane of section was perpendicular to the arteriole (Figure 10). In other instances, necrosis of the PALS was virtually complete, extending from the marginal zone to the central arteriole; in yet other instances, necrosis appeared focally random, extending only to one side of the arteriole. At this stage, nearly all of the germinal centers were necrotic. Viable, large mononuclear cells (resembling lymphoblasts and/or macrophages) were often scattered among the necrotic cells. The spleen from 1 animal contained gram-negative bacteria at this time; bacteria were not found by light or electron microscopy in any lymphoreticular or myeloid tissue of any other hamster in this study.

On Day 2, virus particles were present in most extracellular spaces of the spleen; they were prominent within and adjacent to basement lamina of the vascular bed of the white pulp (Figure 11). Virus particles were also present in necrotic cellular debris and within vacuoles in macrophages and endothelial cells. Phagocytosis of necrotic cellular debris by macrophages was extensive.

By Days 3 and 4 after inoculation, necrosis of the PALS progressed to virtually complete destruction (Figure 12). In all of the animals, the central half of the PALS was necrotic. In half of them, the marginal zone and outer one-fourth to one-half of the PALS contained large mononuclear cells resembling lymphoblasts; this was considered an attempt at repopulation of the white pulp. Except for the more widespread distribution of white pulp necrosis by Day 3, ultrastructural findings were similar to those of Day 2.

Ileum

The course of pathologic events in Peyer's patches of the hamster have been described by Gorelkin *et al.*;[12] these are substantially confirmed by our study. Additional findings not previously reported include productive infection of many intestinal epithelial cells and smooth muscle cells of the muscularis propria. Virus particles were observed budding in moderate numbers from lateral margins of intestinal epithelial cells and accumulating in lateral intercellular spaces (Figure 13). Virions were also observed budding from and lying free between smooth muscle cells. Occasional

flagellate bacilli were observed free in the lamina propria or within PMN phagocytic vacuoles.

Bone Marrow

Bone marrow specimens examined at 8 and 24 hours after inoculation were indistinguishable from normal controls. By Day 2, there was severe necrosis with 75% of the cells in various stages of degeneration. Large areas of nuclear and cytoplasmic debris and pyknotic nuclei contained only few isolated intact cells. Residual cells included myeloid precursors, reticulum cells, and megakaryocytes.

By electron microscopy, virus particles were found budding from plasma membranes of reticulum cells, rubricytes (Figure 14), myeloid precursors (Figure 15), and lymphoblastoid cells (Figure 16). Virus particles were also found free and budding from the lining membranes of platelet demarcation channels of megakaryocytes (Figure 17), and there was apparent damage to these cells. Cytoplasmic vacuoles within some endothelial cells also contained virus particles, as did phagocytic vacuoles within macrophages (Figure 18). Large amounts of cellular debris had also been phagocytosed. The magnitude of this destruction of erythroid, myeloid, and lymphoid cell lines appeared even greater by electron microscopy than by light microscopy.

By Day 3, necrosis involved approximately 90% of the marrow volume. Almost all cells were nucleopyknotic or karyorrhectic, with focal dissolution and apparent removal of the cytolytic debris. The few intact cells remaining included large, poorly differentiated mononuclear cells; some of these resembled reticulum cells, and others resembled lymphoblasts, but most were completely unidentifiable. The ultrastructural findings were similar to those seen on Day 2, with advanced cytonecrosis, presence of viral particles, and phagocytosis of cellular debris by macrophages. At 4 days after inoculation, marrow necrosis was nearly complete. There was marked nucleorrhexis, but a few isolated intact large mononuclear and multinucleate cells persisted, and in 1 animal, intact plasma cells were noted.

Discussion

The extent of the lymphoreticular and myeloid necrosis observed in these hamsters infected with VEE virus was remarkable. At the ultrastructural level of resolution, involvement was seen to be even greater, with hardly a cell in the target organs remaining intact by the time the host animal was moribund. Our findings that the necrotic lesions in lymphoreticular organs at first had a definite topographic distribution and had a

predictable chronologic course of development must be explained in terms of the relative susceptibility of the various cell types in these organs. The initial change in the thymus, that is, the necrosis of randomly distributed individual cells, could not be attributed to a particular susceptibility of any individual cell type because this change was not detected ultrastructurally. Because of the location of thymic epithelial reticular cells in a pericapillary position analogous to that of astroglia in the central nervous system, these cells may have received the first virus from the blood.[18] We have studied lymphoreticular infection with another virus, Tamiami virus, in the spleen, thymus, and lymph nodes of the cotton rat *(Sigmodon hispidus);* in this model, initial viral invasion of reticulum "feeds" subsequent lymphoid infection.[19] No such precise temporal separation of stages was evident in the present study of VEE virus lymphoreticulotropism; however, Gorelkin and Jahrling [12] stated that reticular cell infection preceded lymphocyte infection in Peyer's patches of VEE virus–infected hamsters.

During the major phase of expansion of focalized necrotic lesions in the thymus (Day 2), it was clear that susceptibility and resistance were not related to cell type. The small necrotic foci in both the cortex and medulla involved contiguous epithelial reticular and thymic lymphocytes alike, and destructive events appeared to progress equally in both cell types. The precise demarcation between affected cells and normal cells at the edge of these foci, irrespective of the cell type present at the demarcation, provides further evidence that the viral necrotic process is unselective in nature. Focalization of lesions is considered to be a consequence of cell-to-cell spread of an infectious agent; when the mechanism of VEE shedding from infected cells (by budding from plasma membrane before cell destruction) and the usual speed and magnitude of this viral replicative process are considered, it is remarkable that any focalization of necrosis should have been seen at any stage of disease. Terminally, the confluence of necrotic foci and the presence of virus in all interstitial spaces in the thymus indicate the failure of any potential barriers to viral spread.

Consonant with these destructive effects of VEE virus infection in thymus was the demonstration of the highest infectivity titers in this organ. The thymus has been shown to be the first organ to yield detectable VEE virus after peripheral inoculation of mice—virus has been detected only 2 hours after inoculation.[8] Thus, it is apparent that this organ has a significant role in the course of infection in experimental animals, and this tropism should be adequately studied in species infected in nature.

Distribution of the initial necrotic lesions in the subcapsular cortex of lymph nodes would be more understandable if viral access were known to

be solely via afferent lymphatics which drain into the subcapsular sinus. Virus would, in this case, initially contact lymphoid cells at the outer part of the cortex. However, hematogenous viral access to lymph nodes should result in a random distribution like that seen in thymus. The scattered nucleopyknosis of plasma cells and nucleorrhexis observed in lymph node medullary cords in animals on Day 2 after inoculation may, in fact, be explained in this manner, since each medullary cord is supplied with large amounts of blood from its central blood vessel.[20] There was no apparent selective sensitivity of any particular cell type in lymph node parenchyma. The tendency for necrosis to occur in the periphery of the splenic PALS correlates with the site of initial presentation of hematogenous virus via the capillaries of the marginal zone of the PALS fed from branches of the central arteriole.[21] The subsequent spread of necrosis to the center of the PALS appeared to represent contiguous expansion of foci from the peripheral half of the PALS.

Necrosis of effector cells of the cell-mediated and antibody-mediated immune systems (T and B cells, respectively) and of the cells of the reticuloendothelial system (macrophages) would have profound effects on VEE virus host species which survived acute infection. Necrosis of thymic lymphocytes and epithelial reticular cells could produce the same effects as adult thymectomy. Effects could be more like thymectomy plus whole body irradiation, since T cells in the splenic PALS and in the paracortical region of lymph nodes are among the cells also destroyed by the viral infection. Antibody-forming capacity would be compromised by the destruction of areas rich in B cells, such as lymph node cortex, splenic germinal centers, and Peyer's patches. In fact, VEE infection of hamsters has been compared with radiation necrosis,[22] and studies in mice and in guinea pigs of sublethal VEE virus infection (with an attenuated virus strain) have shown depression of primary antibody response to an antigen given just before the virus.[23,24] On the other hand, mice receiving a foreign antigen after recovery from temperate VEE virus infection produced higher antibody titers than controls.[23] The mice exhibiting this "adjuvant effect" were in a stage of "proliferation of pale, relatively big cells." This may have been a parallel or progression from the peripheral PALS lymphoblastoid repopulation attempt observed in some hamsters on Days 3 and 4 postinfection in this study. The source of these large lymphoblastoid cells in the splenic PALS at a time when the central lymphoid organs, thymus, and bone marrow were still undergoing active, extensive necrosis is certainly puzzling.

Altered reticuloendothelial function in hamsters infected with VEE virus has been demonstrated, and consequent increased susceptibility to

endotoxin-induced shock has been hypothesized by Gorelkin and Jahrling [12] as the cause of death. Some of our observations are consistent with this hypothesis: gram-negative bacteria were present in only 1 animal examined (by special staining technique) during the course of infection; thus, it is most likely that endotoxemia occurs late, and its effects are amplified to a significant level by the preceding pathogenetic events in the reticuloendothelial organs. The observed circulating cytonecrotic debris may have played as important a role in RE blockade as the macrophage necrosis seen in bone marrow, lymph node, and spleen. Definitive proof of the role of endotoxin shock in VEE virus infection should include Limulus assays for circulating endotoxin levels and exogenous endoxtoxin challenge at early stages in the course of infection in an attempt to accelerate or magnify the hypothetical shock death syndrome.

References

1. Murphy FA, Whitfield SG: Eastern equine encephalitis virus infection: Electron microscopic studies of mouse central nervous system. Exp Mol Pathol 13:131–146, 1970
2. Murphy FA, Taylor WP, Mims CA, Marshall ID: Pathogenesis of Ross River virus infection in mice. II. Muscle, heart, and brown fat lesions. J Infect Dis 127:129–138, 1973
3. Austin FJ, Scherer WF: Studies of viral virulence. I. Growth and histopathology of virulent and attenuated strains of Venezuelan encephalitis virus in hamsters. Am J Pathol 62:195–210, 1971
4. Jahrling PB, Scherer WF: Histopathology and distribution of viral antigens in hamsters infected with virulent and benign Venezuelan encephalitis viruses. Am J Pathol 72:25–38, 1973
5. Dill GS, Pederson CE Jr, Stookey JL: A comparison of the tissue lesions produced in adult hamsters by two strains of avirulent Venezuelan equine encephalomyelitis virus. Am J Pathol 72:13–24, 1973
6. Victor J, Smith DG, Pollack AD: The comparative pathology of Venezuelan equine encephalomyelitis. J Infect Dis 98:55–66, 1956
7. Gleiser CA, Gochenour WS, Berge TO, Tigertt WD: The comparative pathology of experimental Venezuelan equine encephalomyelitis infection in different animal hosts. J Infect Dis 110:80–97, 1962
8. Tasker JB, Miesse ML, Berge TO: Studies on the virus of Venezuelan equine encephalomyelitis. III. Distribution in tissues of experimentally infected mice. Am J Trop Med Hyg 11:844–850, 1962
9. Kundin WD: Pathogenesis of Venezuelan equine encephalomyelitis virus. II. Infection in young adult mice. J Immunol 96:49–58, 1966
10. Kissling RE, Chamberlain RW, Nelson DB, Stamm DD: Venezuelan equine encephalomyelitis in horses. Am J Hyg 63:274–287, 1956
11. Monath TP, Calisher CH, Davis M, Bowen GS, White J: Experimental studies of rhesus monkeys infected with epizootic and enzootic subtypes of Venezuelan equine encephalitis virus. J Inf Dis 129:194–200, 1974
12. Gorelkin L, Jahrling PB: Virus-initiated septic shock: Acute death of Venezuelan encephalitis virus-infected hamsters. Lab Invest 32:78–85, 1975
13. Gorelkin L, Jahrling PB: Pancreatic involvement by Venezuelan equine encephalomyelitis virus in the hamster. Am J Pathol 75:349–362, 1974

14. Chappell WA, Sasso DR, Toole RF, Monath TP: Labile serum factor and its effect on arbovirus neutralization. Appl Microbiol 21:79–83, 1971
15. Mollenhauer HH: Plastic embedding mixtures for use in electron microscopy. Stain Technol 39:111–114, 1964
16. Venable JH, Coggeshall R: A simplified lead citrate stain for use in electron microscopy. J Cell Biol 25:407–408, 1965
17. Walker DH, Harrison A, Murphy K, Flemister M, Murphy FA: Unpublished data
18. Greep RO, Weiss L: Histology, New York, McGraw-Hill, 1973
19. Murphy FA, Winn WC Jr, Walker DH, Flemister MR, Whitfield SF: Early lymphoreticular viral tropism and antigen persistence: Tamiami virus infection in the cotton rat. Lab Invest 34:125–140, 1976
20. Yoffey JM, Courtice FC: Lymphatics, Lymph and the Lymphomyeloid Complex. London, Academic Press, Inc., Ltd., 1970
21. Weiss L: The Cells and Tissues of the Immune System: Structure, Functions, and Interactions. Englewood Cliffs, N.J., Prentice-Hall, 1972
22. Gochenour WS: The comparative pathology of Venezuelan encephalitis virus infection in selected animal hosts. Proceedings of the Workshop-Symposium on Venezuelan Encephalitis Virus, 1971. Washington, D.C., Pan American Health Organization, 1972 (Scientific Publication No. 243)
23. Hrusková J, Rychterová V, Kliment V: The influence of infection with Venezuelan equine encephalomyelitis virus on antibody response against sheep erythrocytes. I. Experiments on mice. Acta Virol 16:115–124, 1972.
24. Hrusková J, Rychterová V, Kliment V: The influence of infection with Venezuelan equine encephalomyelitis virus on antibody response against sheep erythrocytes. II. Experiments on guinea pigs. Acta Virol 16:125–132, 1972

Dr. Kevin Murphy's present address is Department of Internal Medicine, University of Texas, Southwestern Medical School, 5323 Harry Hines Boulevard, Dallas, TX 75235.

Use of trade names is for identification only and does not constitute endorsement by Public Health Service or by the US Department of Health, Education, and Welfare.

[*Illustrations follow*]

All light micrographs are of sections stained with hematoxylin and eosin. All electron micrographs are of sections stained with uranyl acetate and lead citrate.

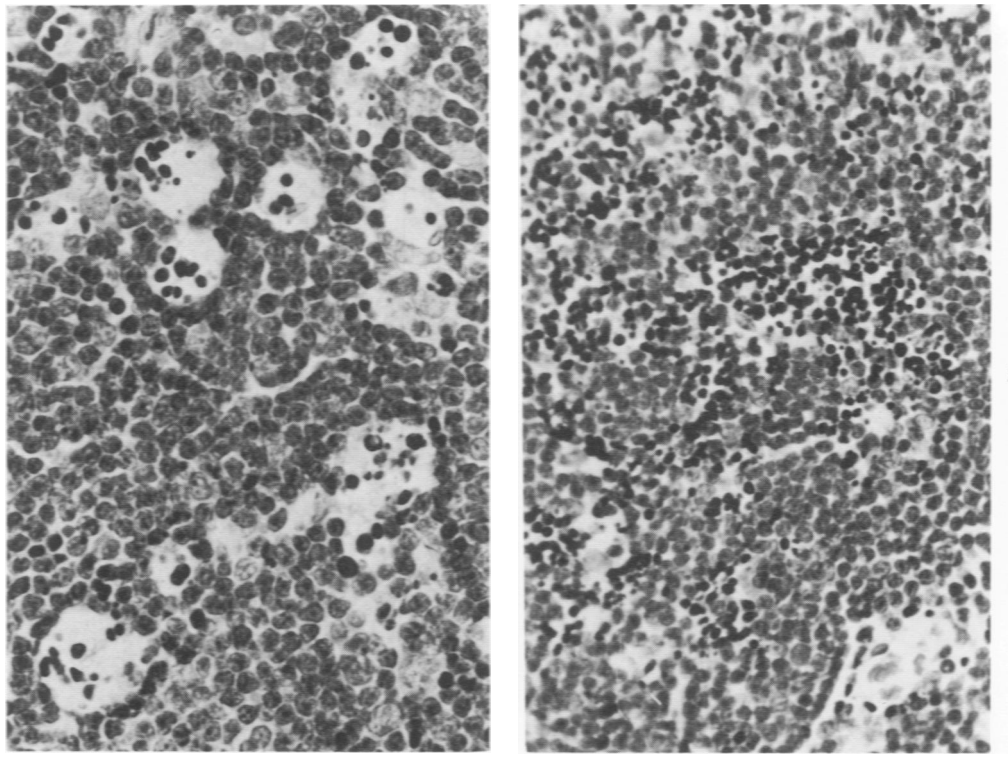

2

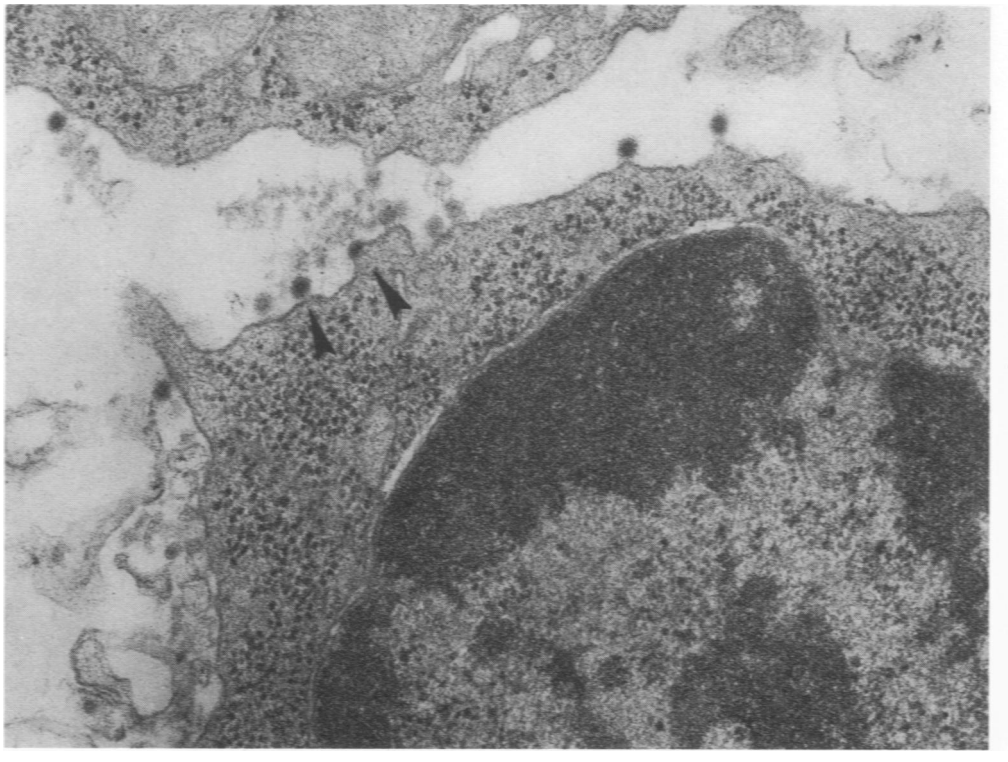

3

Figure 1—Thymus, 2 days postinoculation. Focal lesions consist of rounded, "punched out" foci of cells with pyknotic nuclei intermixed with nucleorrhectic debris and lucent space. (× 440) **Figure 2**—Thymus, 2 days postinoculation. Focal lesions consist of irregular pyknotic cells without lucent surrounding space or precise separation from normal surrounding cells. (× 270) **Figure 3**—Thymus, 2 days postinoculation. Typical VEE virus particles (*arrows*) are budding from the plasma membrane of a thymocyte. (× 45,600)

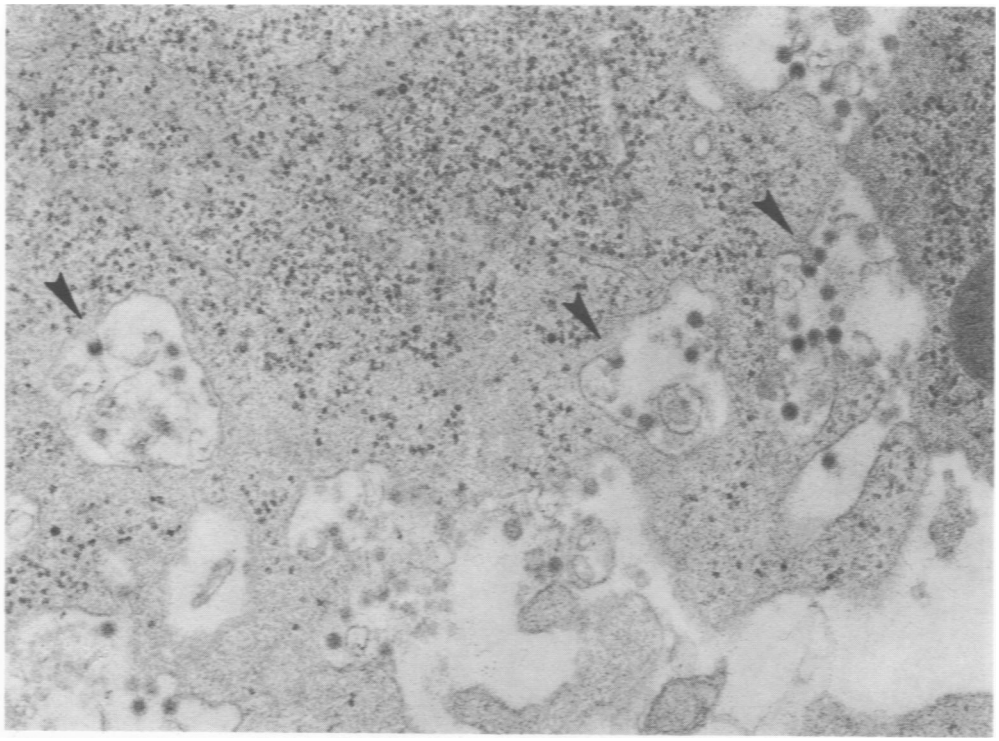

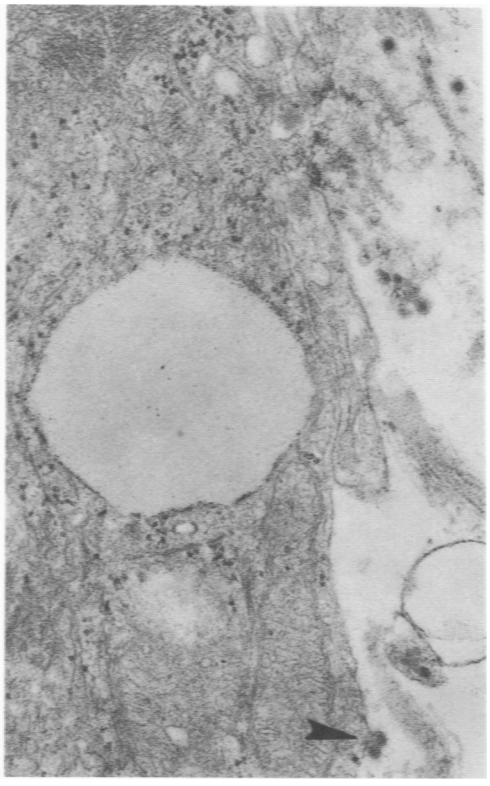

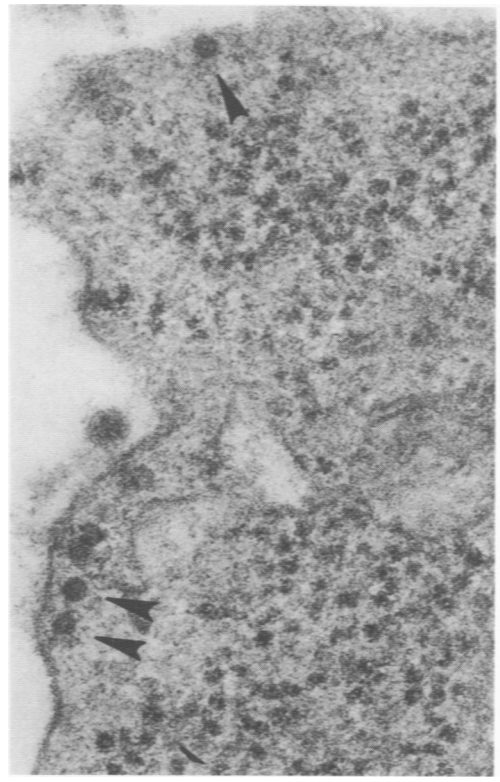

Figure 4—Thymus, 2 days postinoculation. Virus particles (*arrows*) are budding upon large lymphoblastoid cell (× 42,900) **Figure 5**—Thymus, 2 days postinoculation. Infection of epithelial reticular cells was evidenced by viral budding (*arrow*). (× 34,600) **Figure 6**—Thymus, 2 days postinoculation. VEE nucleocapsids (*arrows*) are in the cytoplasm adjacent to the plasma membrane of a small thymocyte. (× 91,300)

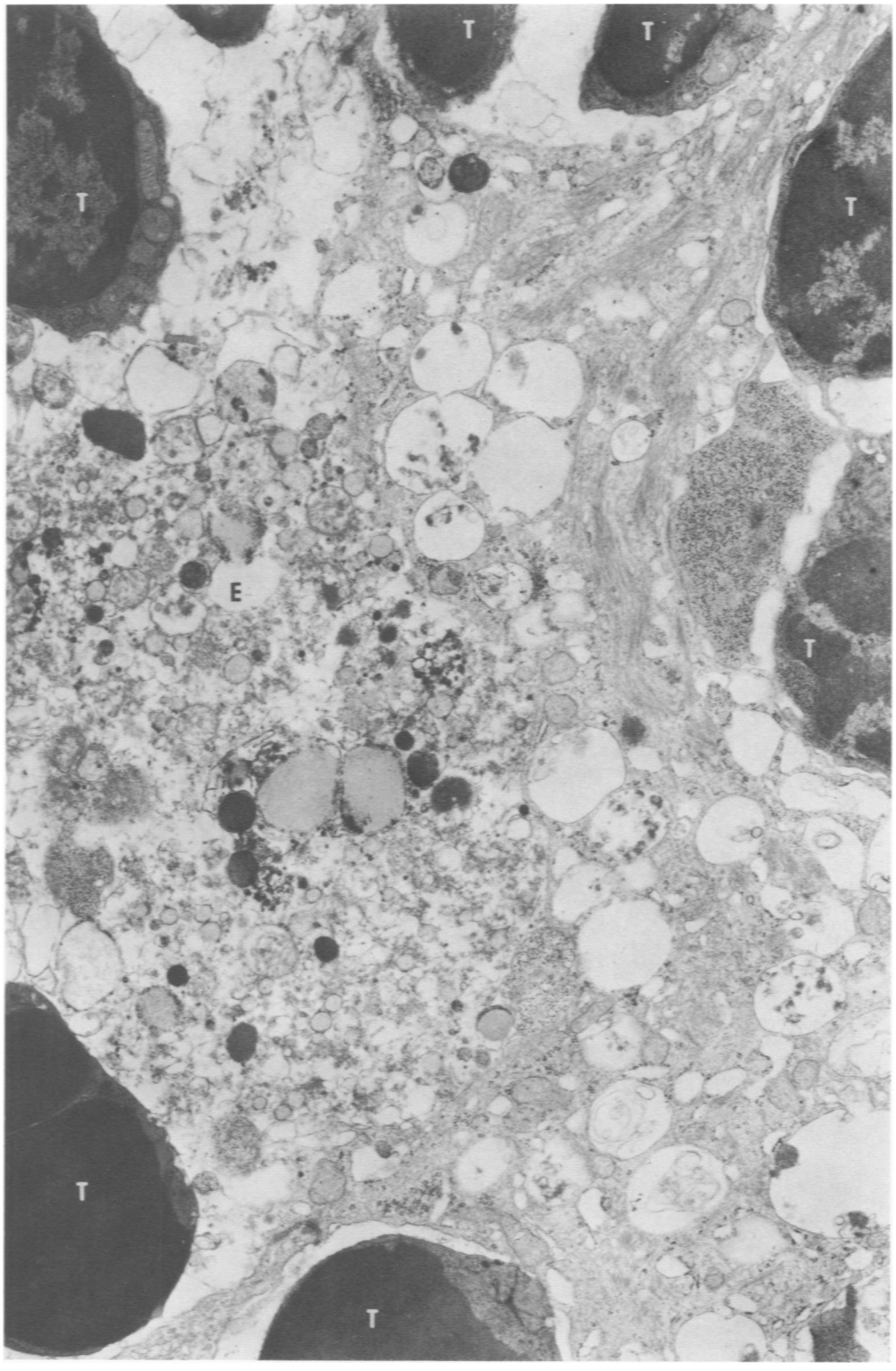

Figure 7—Thymus, 2 days postinoculation. Survey micrograph of necrosis of contiguous cells [epithelial reticular cells (*E*) and thymocytes (*T*)] showing the sharp demarcation between intact and necrotic cells. (× 23,000)

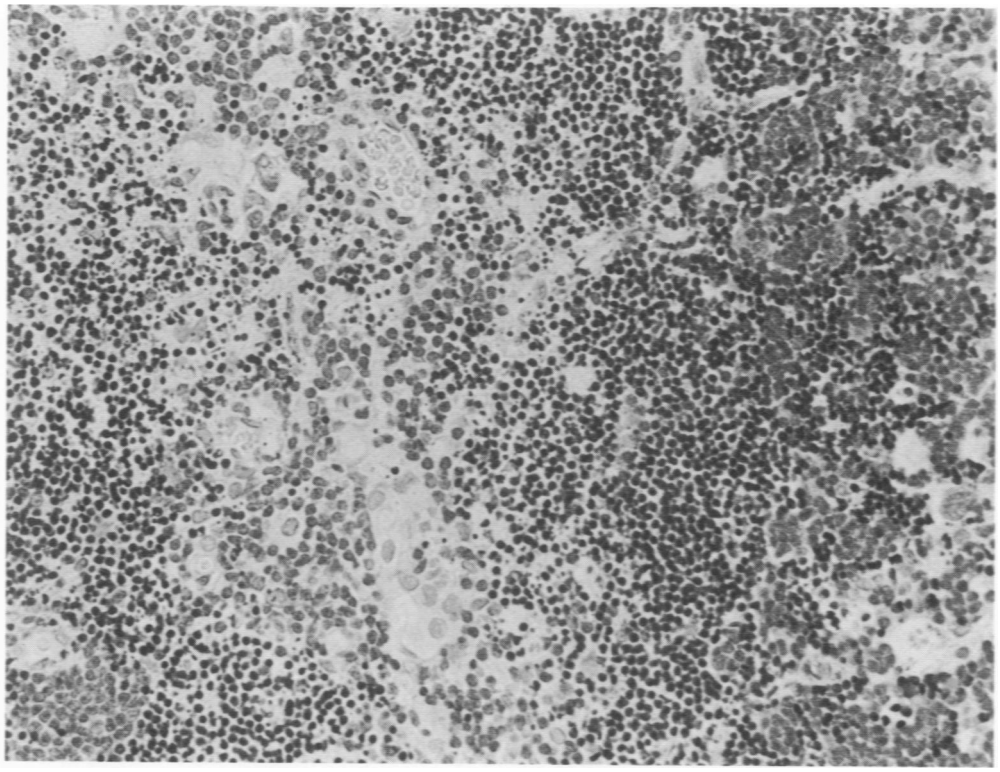

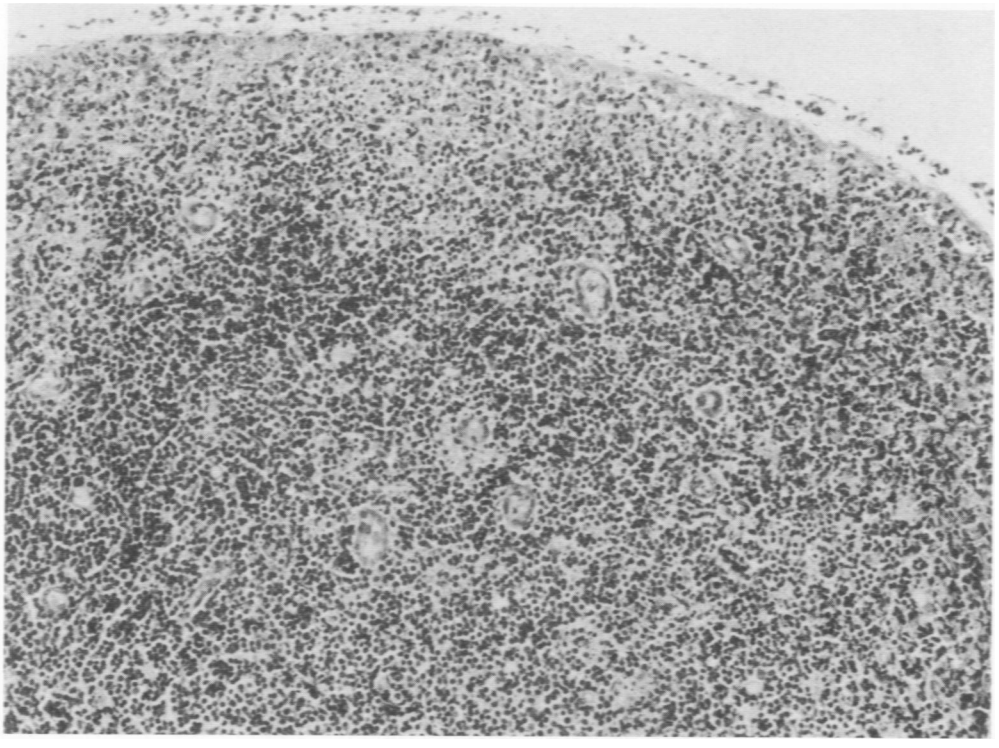

Figure 8—Thymus, 3 days postinoculation. Necrotic changes involve approximately 60% of the mass of the thymus, affecting cortex and medulla and lymphoid and reticular elements uniformly. (× 270) **Figure 9**—Lymph node, 2 days postinoculation. Cortical lymphoid necrosis is confluent, contrasting with the relative sparing of the medullary elements. (× 110)

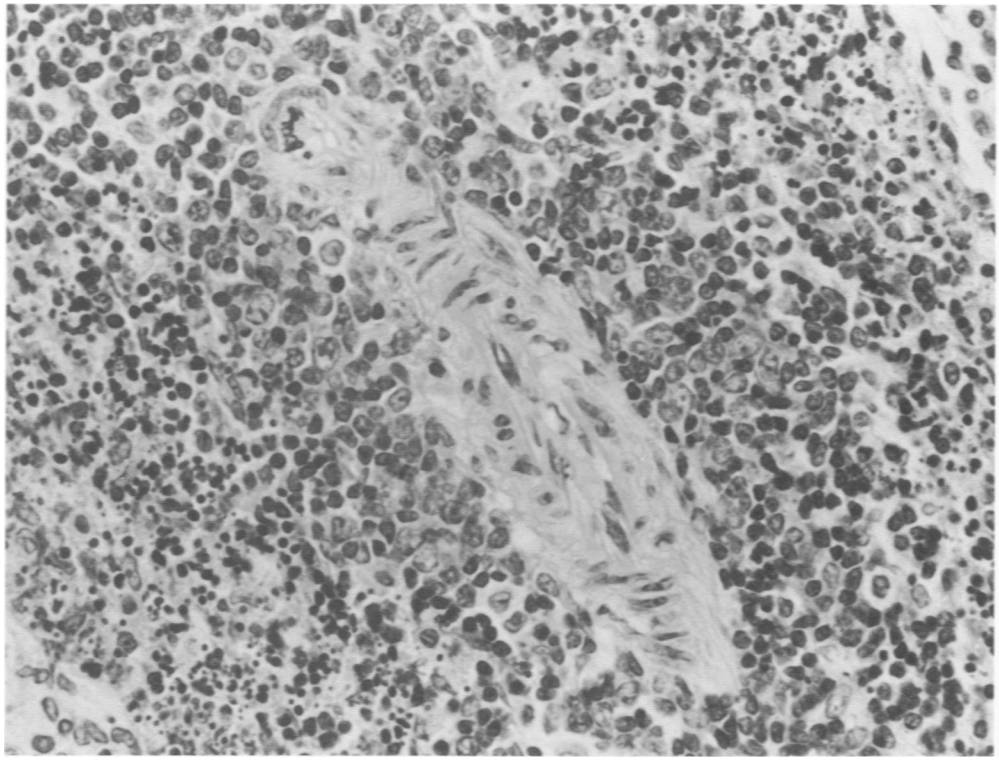

10

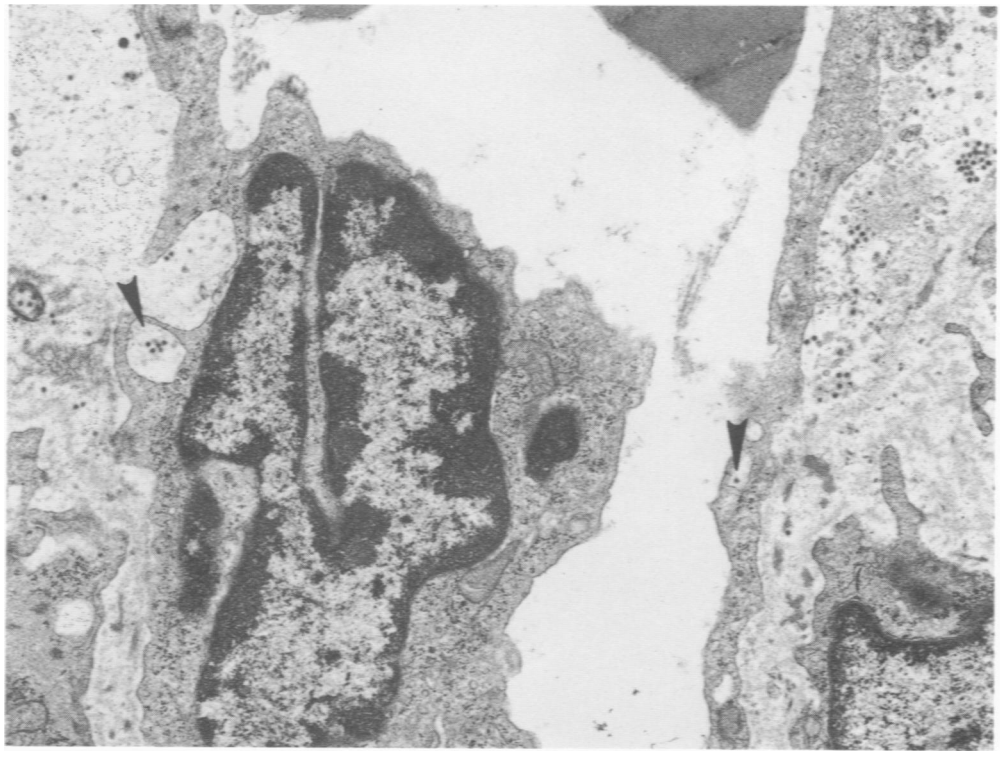

11

Figure 10—Spleen, 2 days postinoculation. Necrosis of cells within the periarteriolar lymphocytic sheath (PALS). (× 140) **Figure 11**—Spleen, 2 days postinoculation. VEE virus particles are prominent both within and adjacent to the basement lamina of the vascular bed of the white pulp and are also within vacuoles in endothelial cells (*arrows*). (× 18,000)

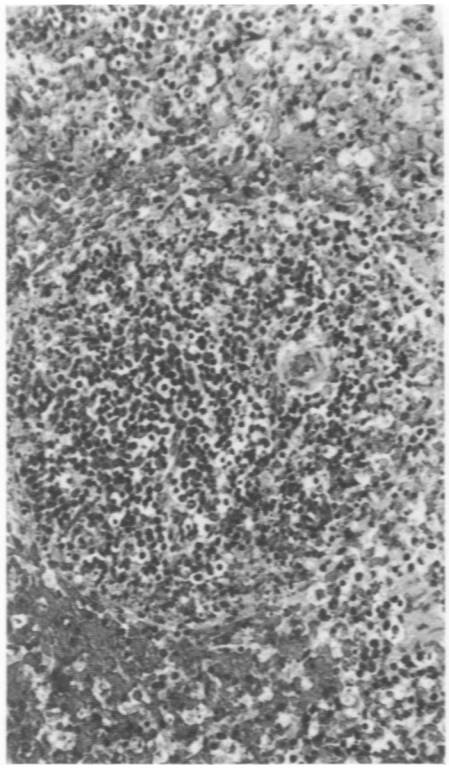

12A

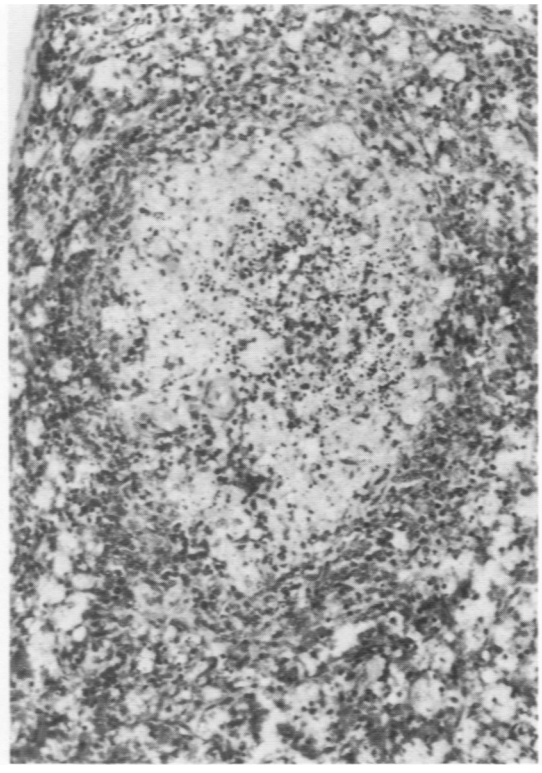

12B

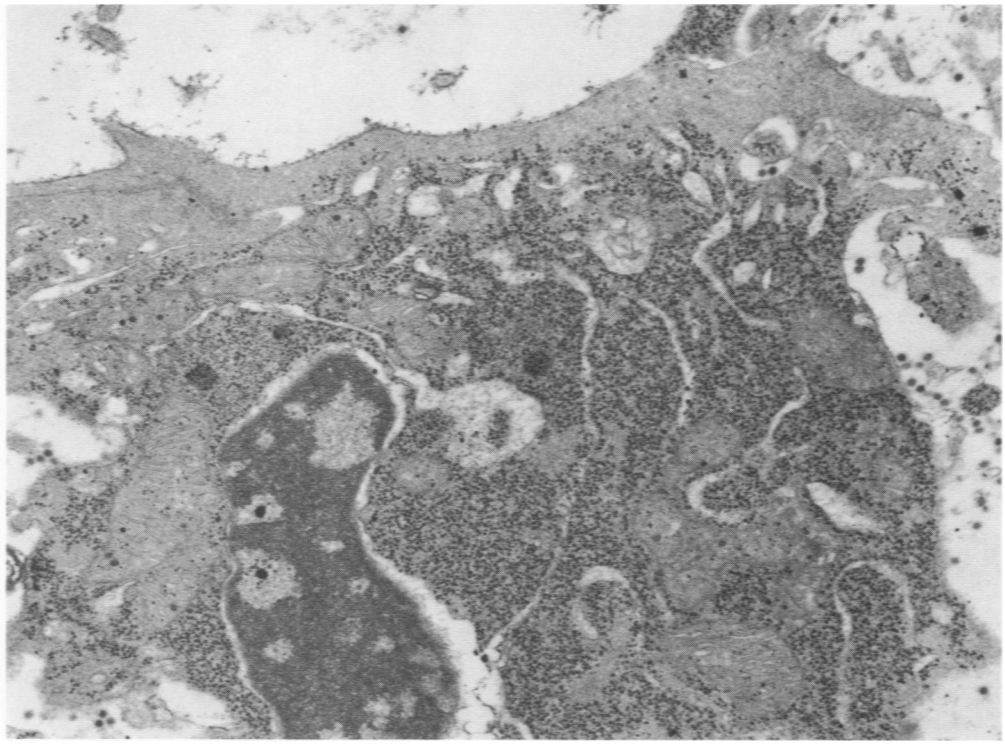

13

Figure 12 A and B—Spleen, 3 days postinoculation. The progress of necrosis of the PALS is evidenced by pyknosis of lymphocytes in all zones (**A**) and finally, by dissolution of these cells, leaving a homogeneous eosinophlic remnant of the PALS (**B**). (×110) **Figure 13**—Ileum, 3 days post-inoculation. Infected intestinal epithelial cells have virus particles budding from lateral margins and accumulating in intercellular spaces (× 18,800)

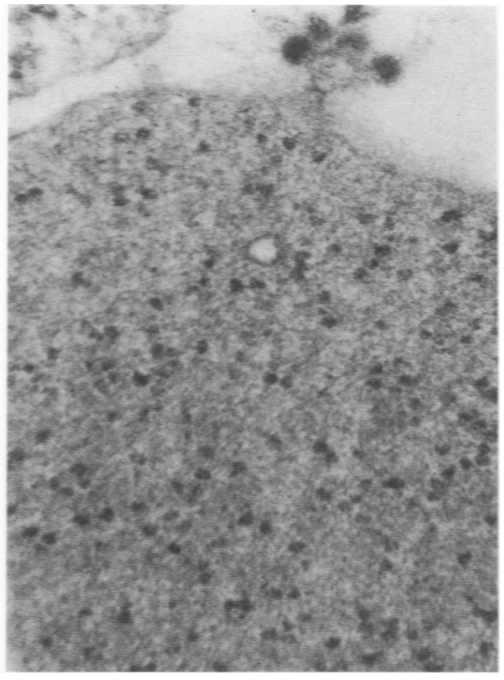

14

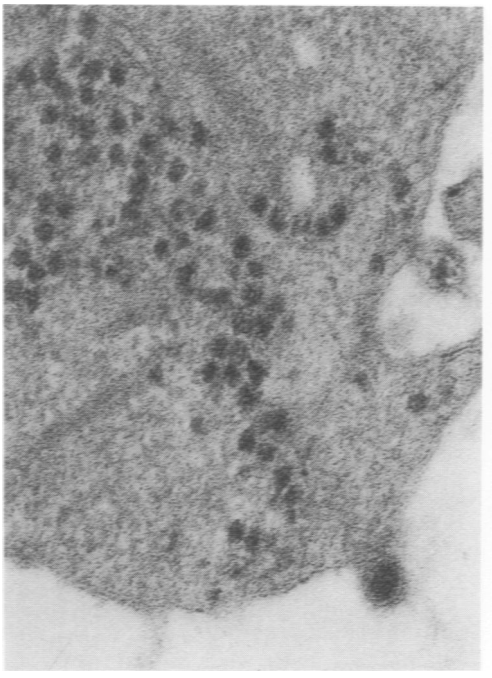

15

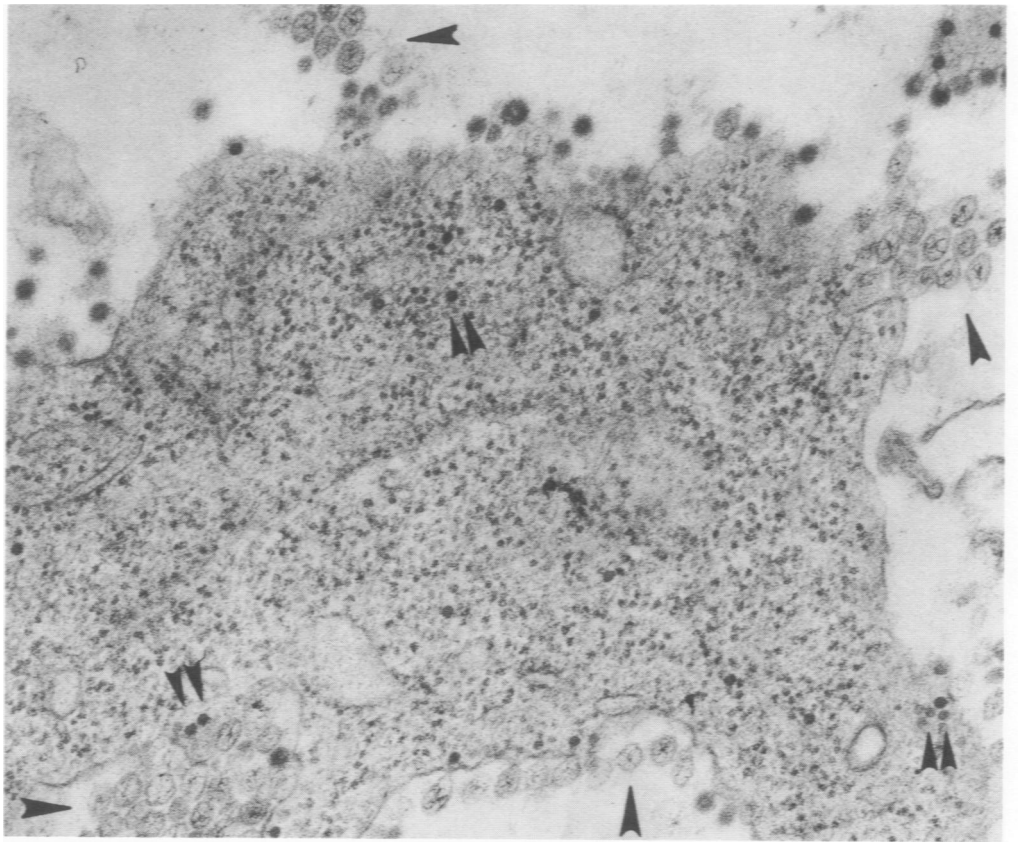

16

Figure 14—Bone marrow, 2 days postinoculation. VEE virus particles are budding from the plasma membrane of a rubricyte. (× 80,800) **Figure 15**—Bone marrow, 2 days postinoculation. VEE virus particle budding from the plasma membrane of a myeloid precursor. (× 127.000) **Figure 16**—Bone marrow, 2 days postinoculation. VEE virus particles and associated spherules (*arrows*) budding from the plasma membrane of a lymphoblastoid cell. Some nucleocapsids (*double arrows*) are present in the cytoplasm (× 56,100)

17

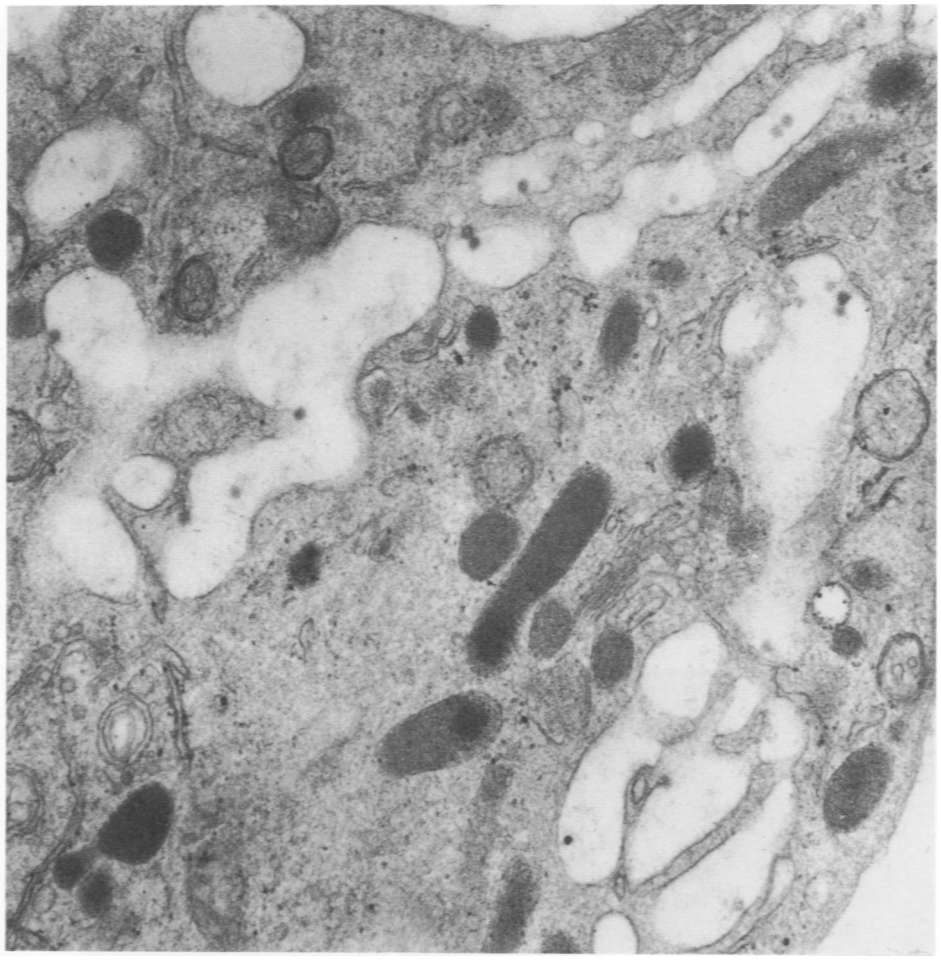

18

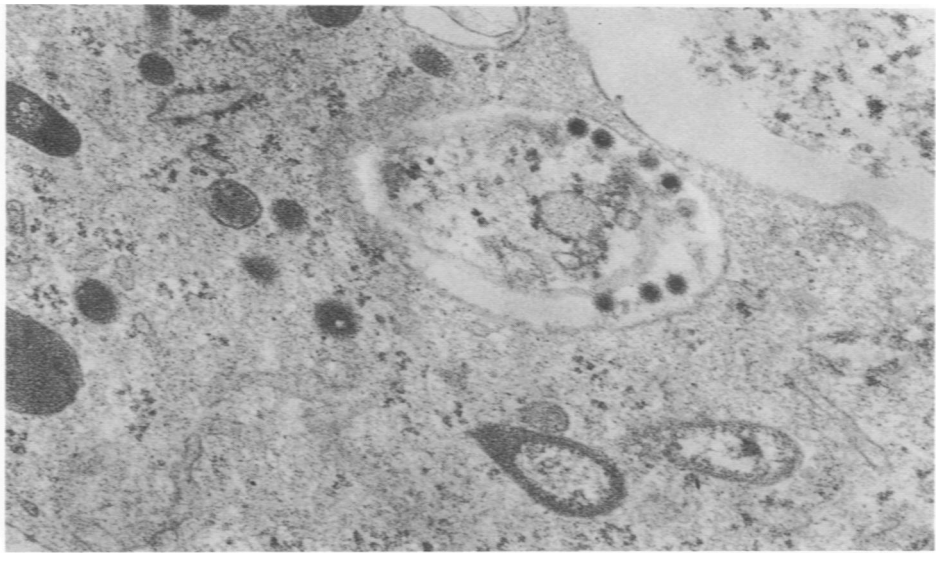

Figure 17—Bone marrow, 2 days postinoculation. Virus particles are free and budding from the lining membranes of platelet demarcation channels of a megakaryocyte. (× 31,200) **Figure 18**—Bone marrow, 2 days postinoculation. Phagocytic vacuole within a macrophage contains virus particles. (× 59,000)